Outer Heliosphere Workshop
Boulder, CO, July 21 – 23, 2021

Multi-component, Multi-scale Interaction of the Solar Wind with the Local Interstellar Medium

N.V. Pogorelov[1,2]

[1]University of Alabama in Huntsville, Department of Space Science
[2]Center for Space Plasma and Aeronomic Research

Contributor List

Federico Fraternale, Tae Kim, Dinesha Hegde, Talwinder Singh, Pete Smith, Mehmet Yalim, Gary Zank, University of Alabama in Huntsville

Charles N. Arge, N. Gopalswamy, NASA GSFC

Leonard F. Burlaga, Donald Gurnett, John Richardson, and the Voyager team

Phillip Colella, Brian Van Straalen, LBNL

Michael Gedalin, Ben-Gurion University of the Negev, Beer-Sheva, Israel

Jacob Heerikhuisen, University of Waikato, New Zealand

Grzegorz Kowal, University of São Paulo, Brazil

Igor Kryukov, Institute for Problems in Mechanics, Russian Academy of Sciences

Vadim Roytershteyn, Space Science Institute, Boulder, CO

Ming Zhang, Florida Institute of Technology

Requirements to the Model Development

1. **Interaction of the local interstellar medium (LISM) with the heliosphere involves MHD discontinuities on multiple scales: Efficient shock-capturing methods should be implemented in an adaptive mesh refinement (AMR) framework.**

2. **LISM is partially ionized: Charge exchange (collisions) between neutral atoms and ions should be taken into account, e.g., through a multi-fluid, multi-component approach.**

3. **Charge exchange events are very infrequent: MHD equations should be coupled with the kinetic Boltzmann equation.**

4. **Charge exchange of LISM atoms with solar wind (SW) ions creates non-thermal ions (pickup ions, PUIs): PUIs should be treated separately, e.g., by solving the Fokker-Planck equation, but simpler models are also used.**

5. **The PUI distribution function is unstable: Generation of turbulence and its interaction with ions should be addressed properly.**

6. **SW is time-dependent on different time scales: Spacecraft data and remote measurements should be used to create the boundary conditions.**

7. **Galactic cosmic ray transport can be simulated using the background plasma. Efficient data extraction is necessary.**

8. **Disparate spatial scales should be resolved for meaningful comparisons with observational data, which results in large data sets: Efficient I/O procedures should be developed and scalable parallelization implemented.**

The Structure of the Multi-Scale Fluid-Kinetic Simulations Suite

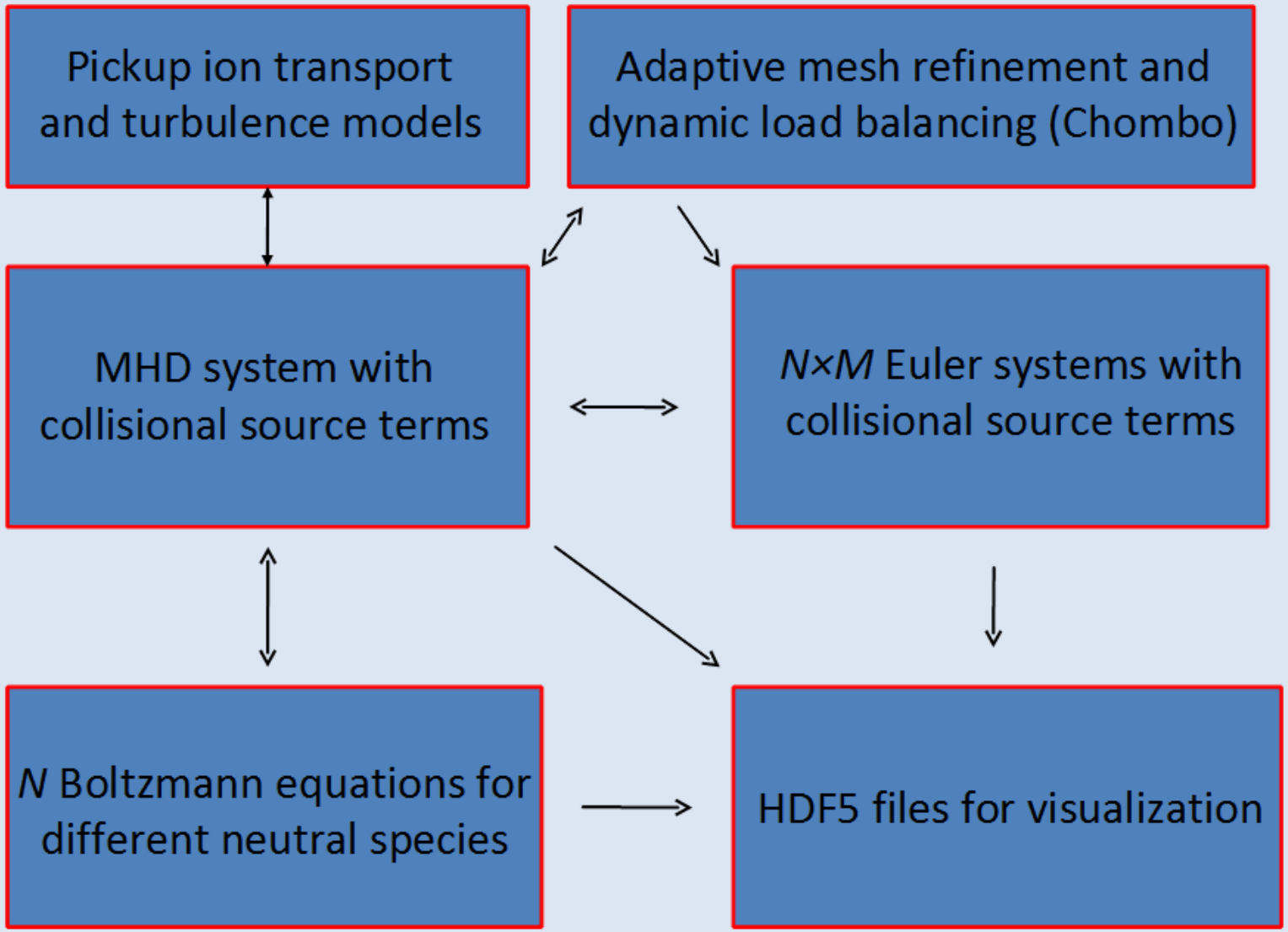

Corotating Interaction Regions

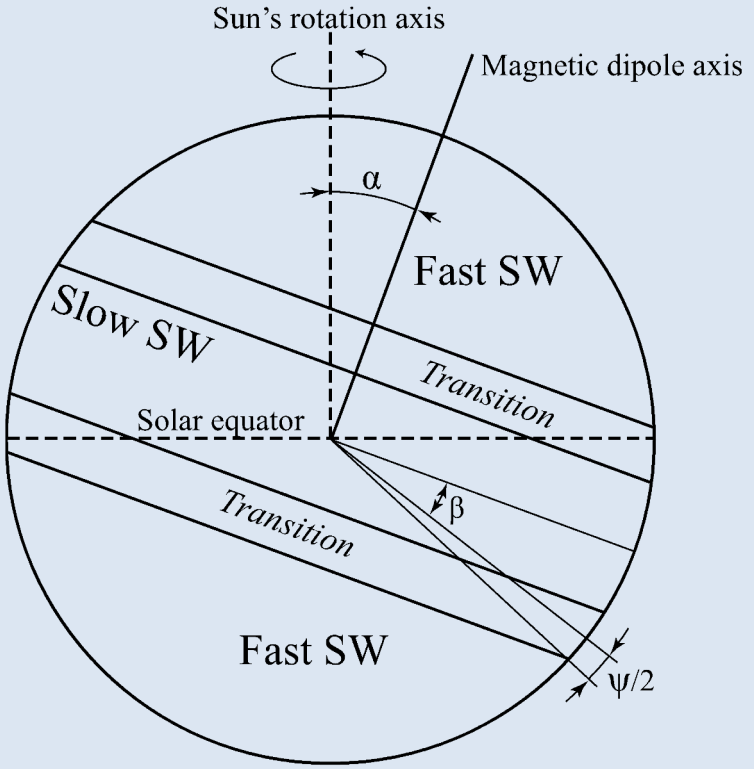

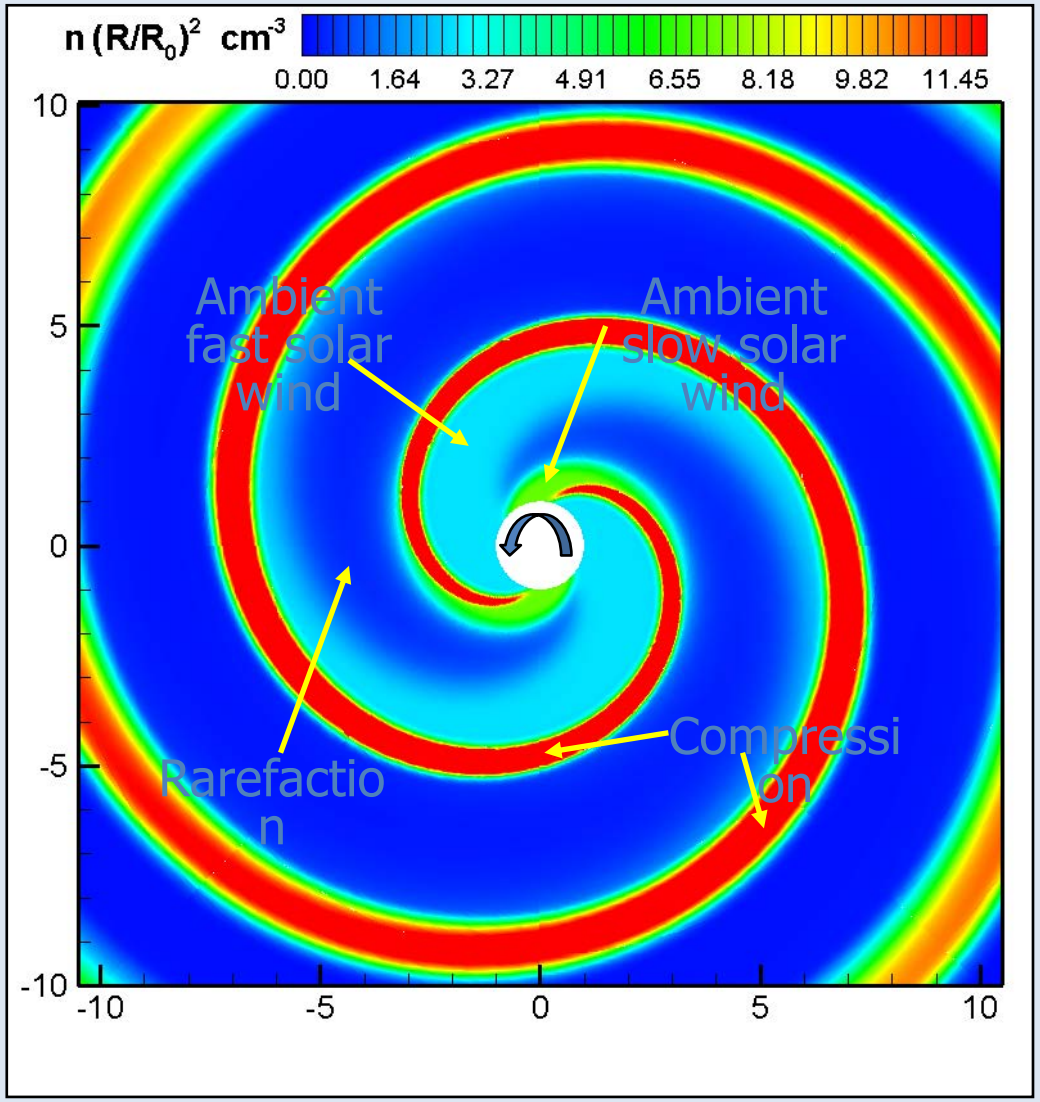

The solar wind during solar minima consists of two types of plasma structures: Fast, low-density, high-temperature plasma flows from regions located at both north and south poles of the magnetic dipole axis, while slow streams originate near the dipole equator. The transition between fast and slow regimes is sharp but not discontinuities.

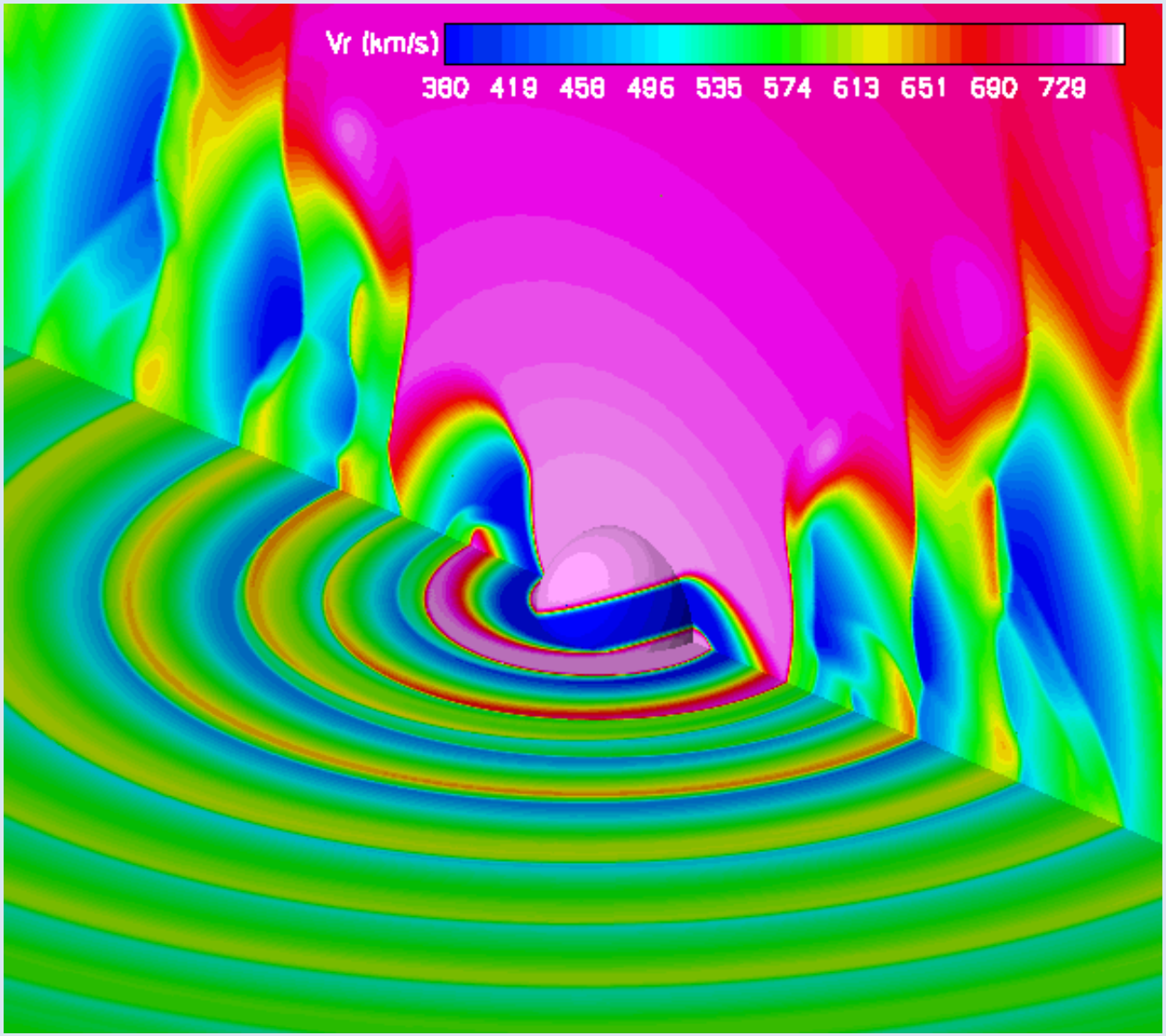

Stream interaction due to solar rotation

MS-FLUKSS applications

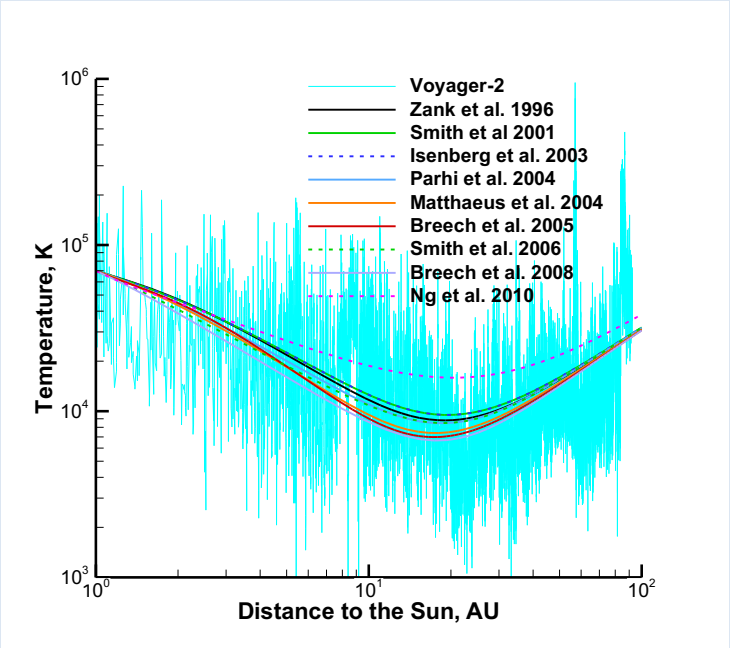

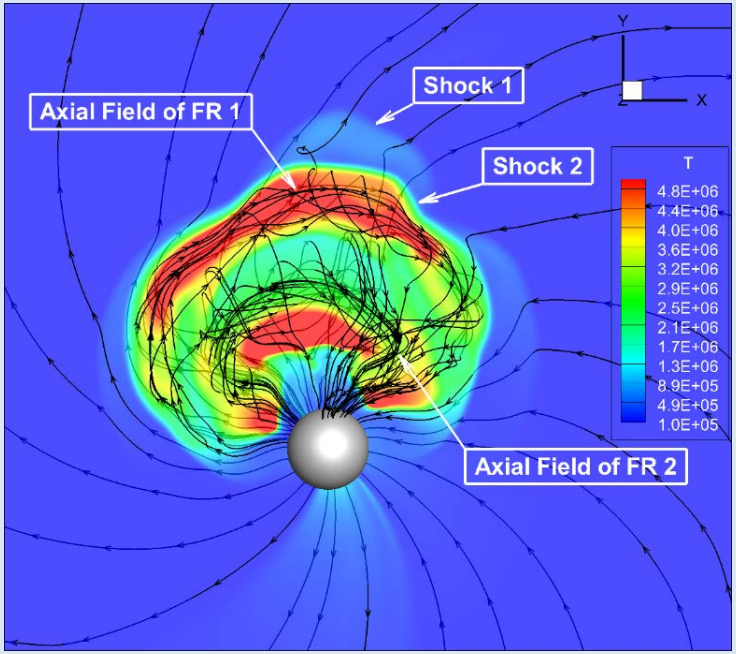

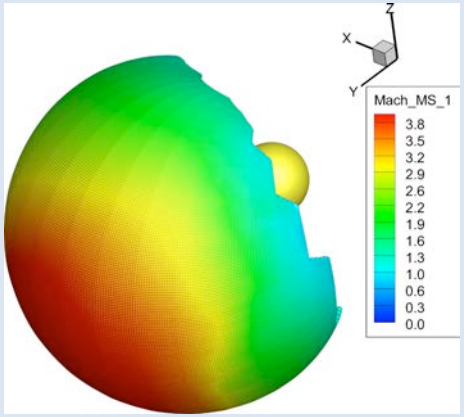

Clockwise: (i) comparison of turbulence models with Voyager data; (ii) interaction of two CMEs; (iii) CME shock surface colored by the fast magnetosonic Mach number.

MORE IN THE NEXT PRESENTATION OF TAE KIM

SW-LISM interaction pattern in the presence of solar cycle effects

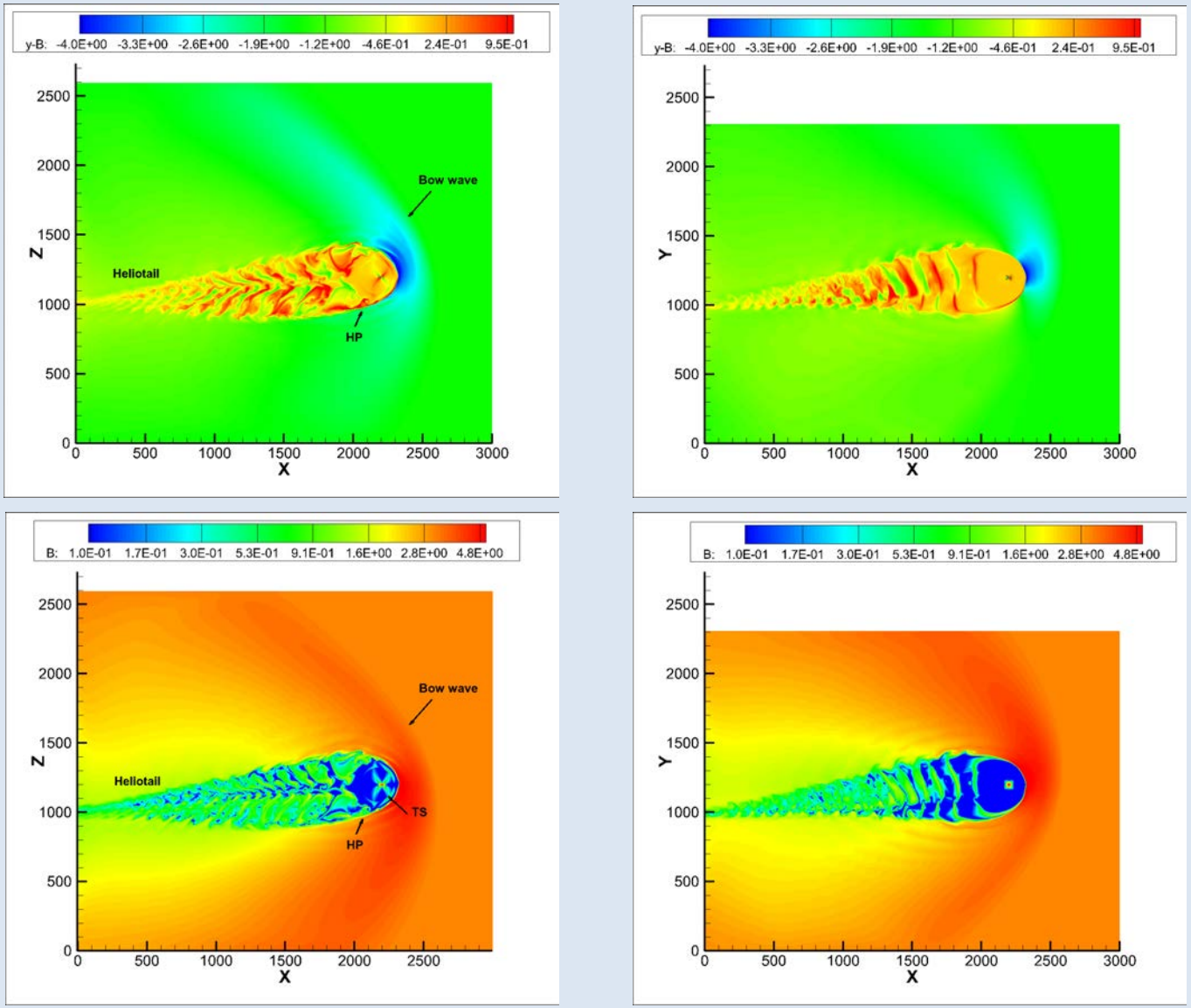

The model reproduces the TS and HP crossings with by V1 and V2 (this one was predicted) with a rather high accuracy (Pogorelov et al., 2013; 2015).

The y-component (top panels) of the magnetic field vector and its magnitude (bottom panels) in the meridional (left panels) and equatorial (right panels) planes. Distances are given in AU and magnetic filed in μG. One can see the TS, HP, and bow wave.

Transition to chaotic behavior in the IHS (Pogorelov et al., 2013)

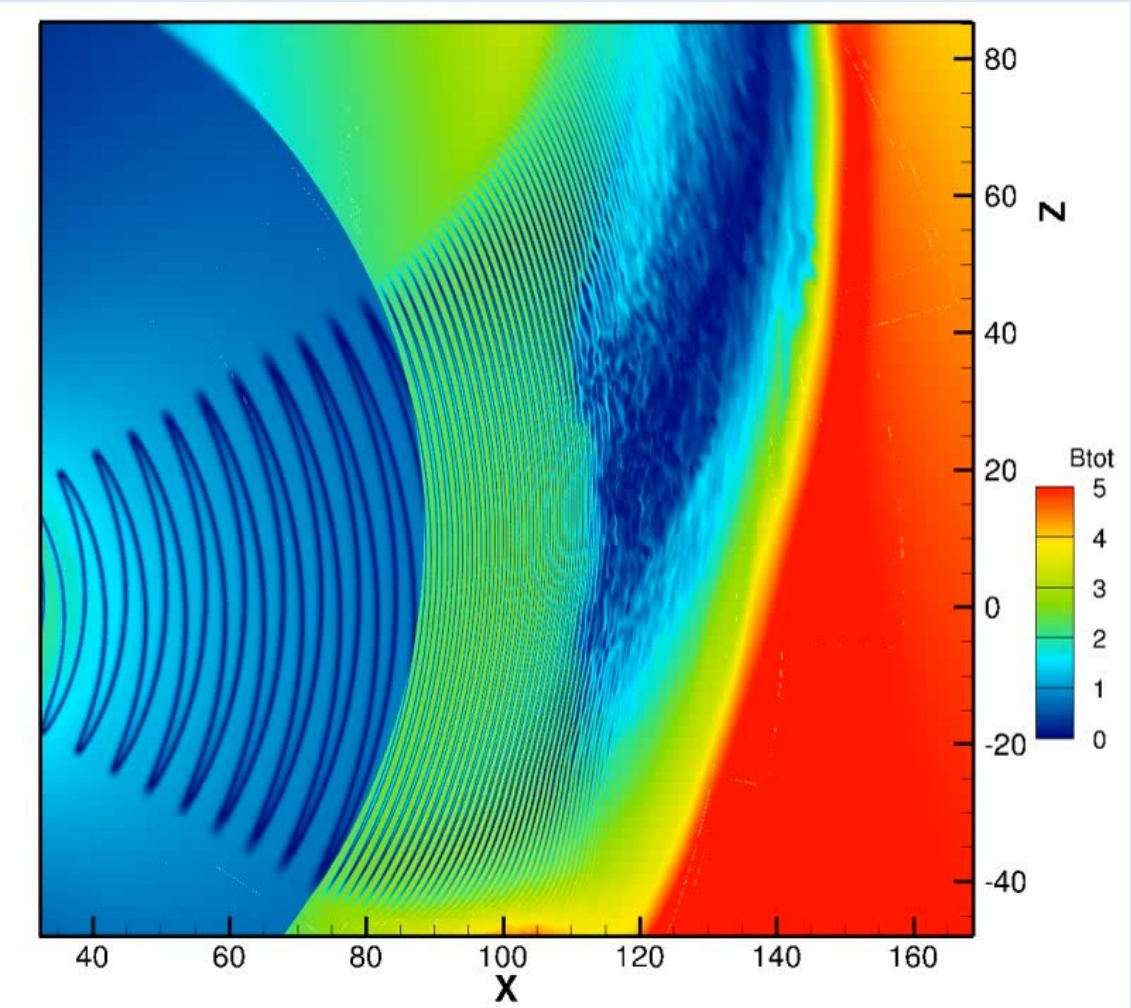

A side note:

Traditional sectors do not exist beyond 10 AU or less.

No standard B-V exhausts have been observed by Voyagers. Involving turbulence may be a fruitful approach, since it produces the multifractal structure that is observed in the magnetic field strength.

Evolution of the heliospheric magnetic field in the inner heliosheath: the reason is tearing-mode instability due to numerical dissipation. In reality, such turbulent behavior is seen everywhere in the IHS.

Deriving the IBEX Ribbon from Numerical Simulations

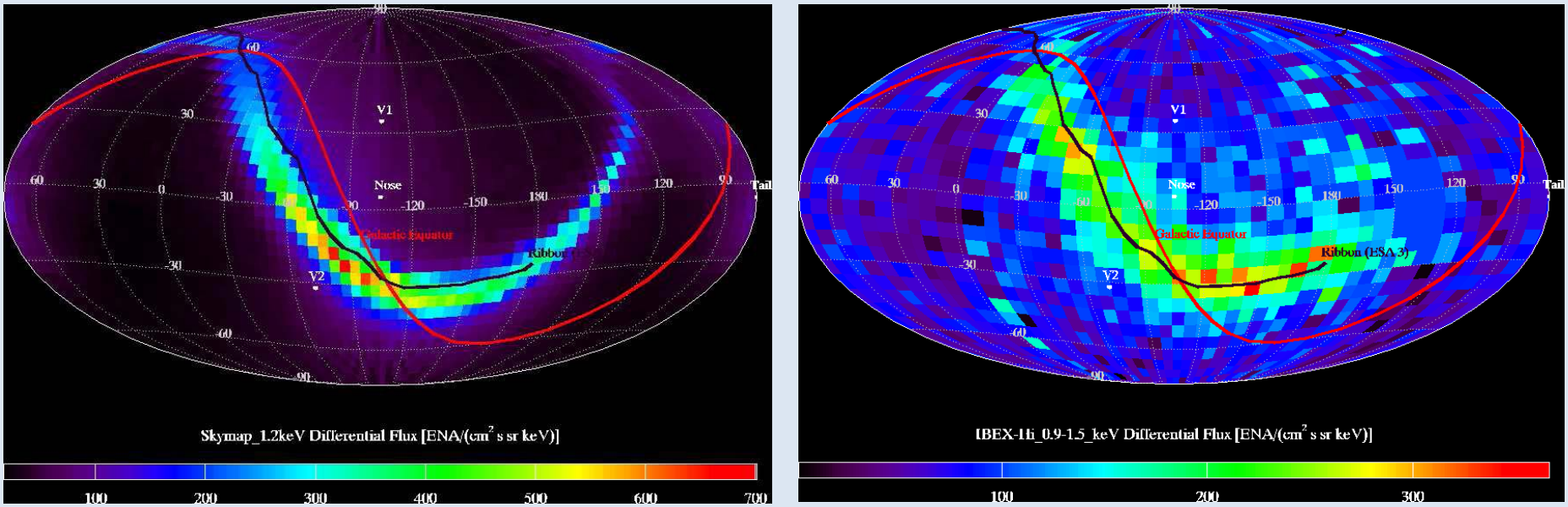

FIGURE 1. All-sky maps of simulated (left) and observed (right) ENA fluxes at 1.1 keV. The simulation uses a $\kappa = 1.63$ spectral index for IHS protons, and we have assumed that all PUIs retain partial shell distributions long enough to re-neutralize before they isotropize. The red curve is the galactic plane, and a best fit to the observed ribbon is shown as a black line. Note that the ribbon shifts down slightly at high energies. Units of ENA flux are $(\text{cm}^2\ \text{s sr keV})^{-1}$.

From Heerikhuisen et al. (2010)

The effect of PUIs treated as a separate fluid and with boundary conditions imposed on them at the termination shock (Pogorelov et al., 2016)

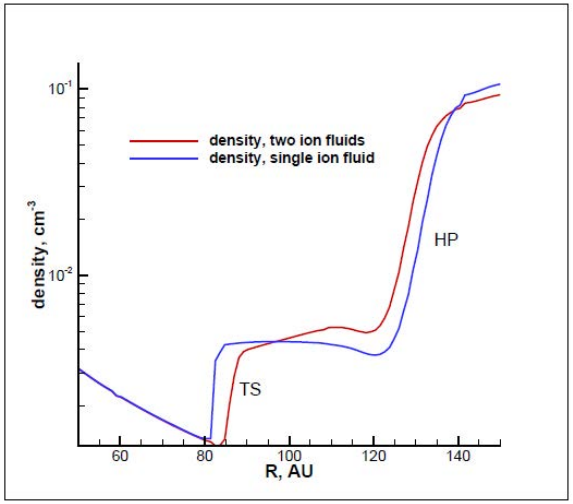

Figure 1. Ion density distributions along the *V1* trajectory shows that the TS moves farther from the Sun while the HP becomes closer to it, if PUIs are treated as a separate plasma component.

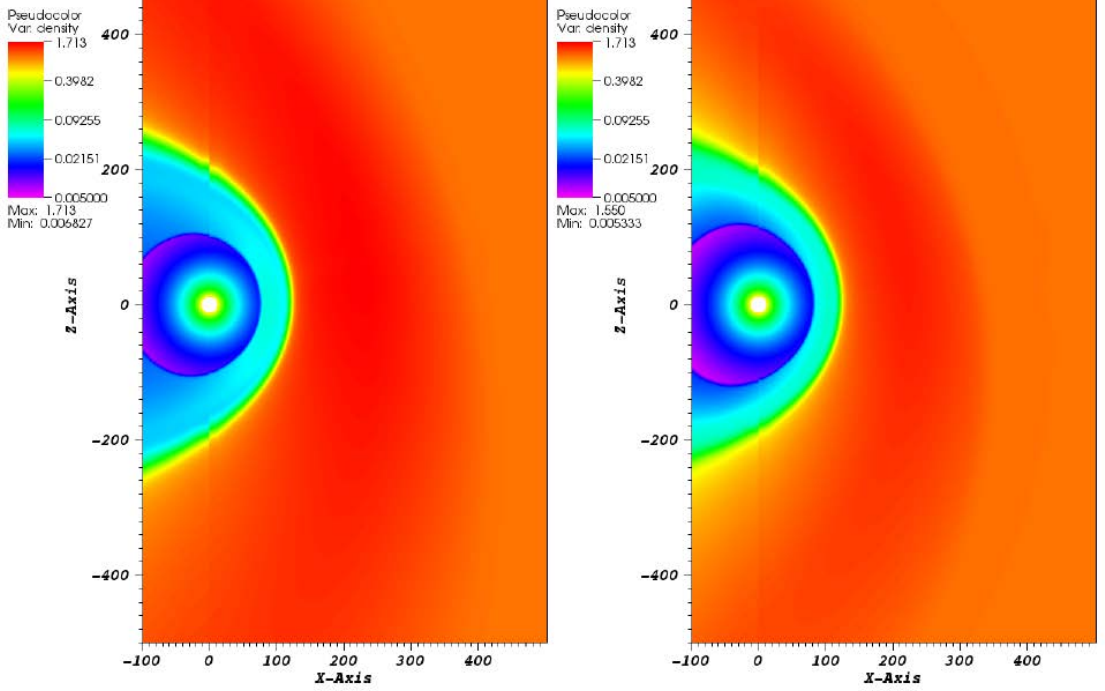

Figure 2. Plasma density distributions in the meridional plane for the single-ion-fluid model (left panel) and for the case when the PUI and thermal ion fluids behave as co-moving, but distinguishable components (right panel)

The IHS shrinks if PUIs are treated as a separate fluid. However, the effect of decreasing SW ram pressure is likely to be of more importance. Unfortunately, there is no way to find out where the TS is located now.

Boundary conditions at collisionless shocks

- SW-LISM interactions performed so far have been using either highly approximate or NO boundary conditions for PUIs at the termination shock.
- Our aim is to use kinetic simulations to derive such boundary conditions and use them in global simulations.

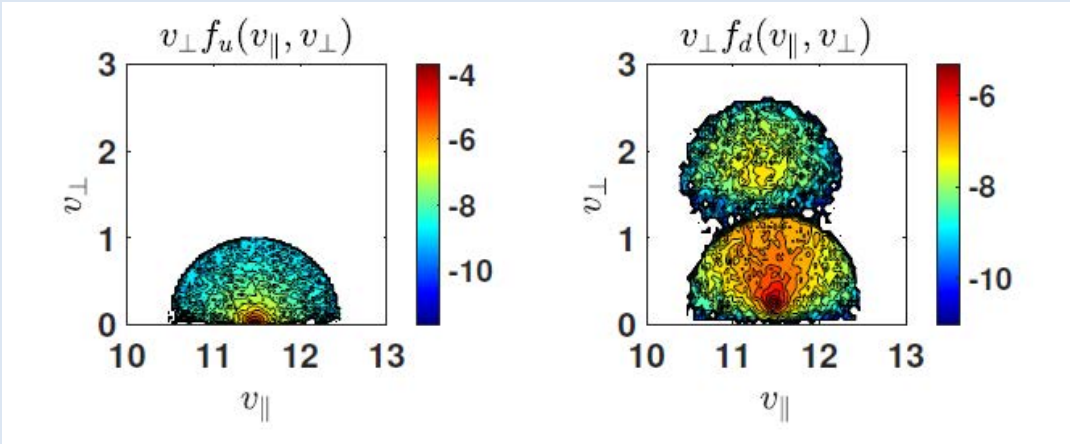

The upstream and downstream distributions of PUI for B_d/B_u = 2.7 and θ_u = 85°. Directly transmitted and those reflected once and proceed further downstream afterwards. 22% of PUIs are reflected, i.e., higher than due to the cross-shock potential only. The downstream perpendicular temperature of reflected PUIs is an order of magnitude lower than it was predicted by a number of authors earlier. **From Gedalin et al. (2021).**

Helium in the Heliosphere (in addition to H) (Fraternale et al., 2021)

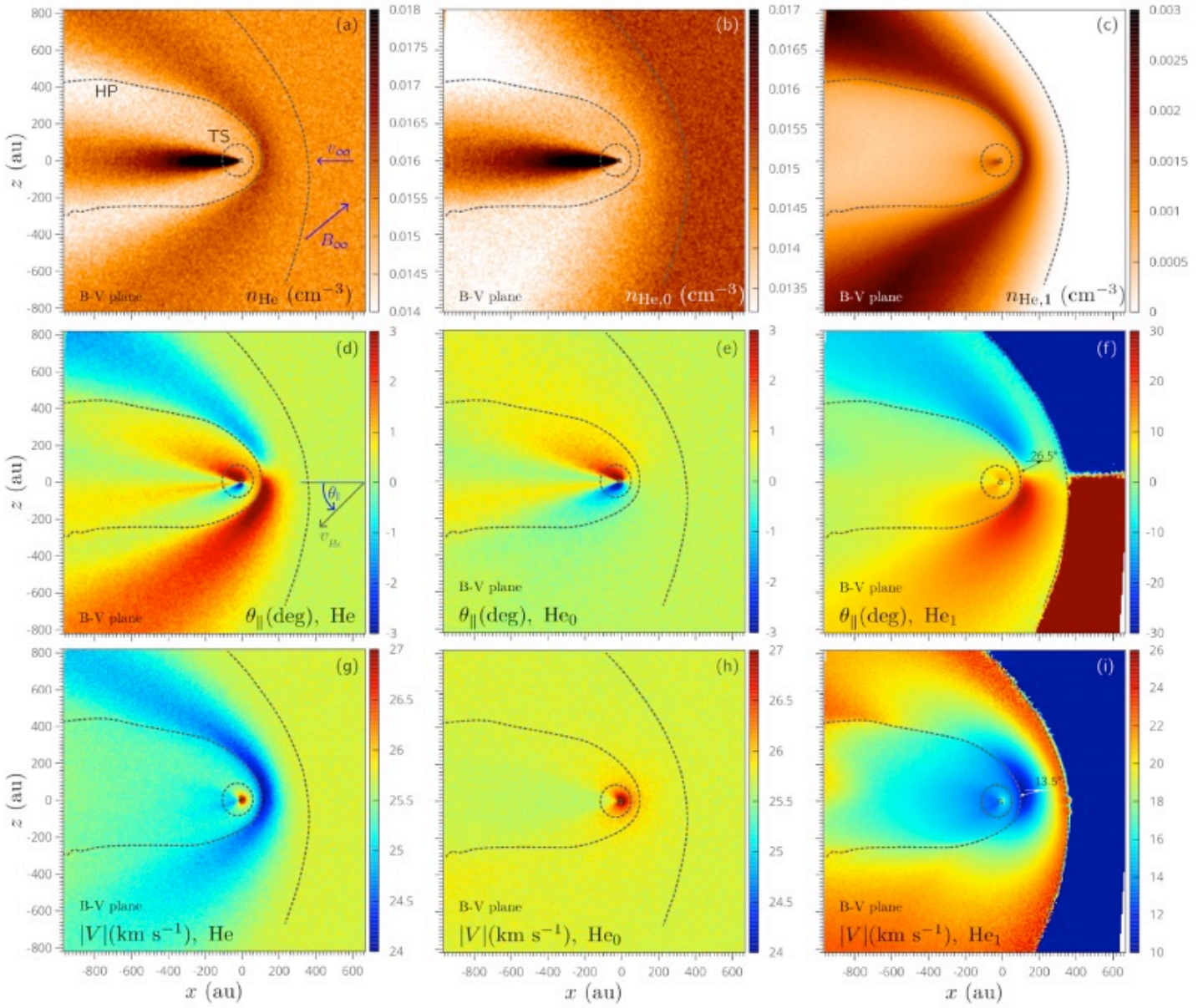

Figure 1. ISN He distributions in the B-V plane. From the top to the bottom, the average number density, in-plane deflection, and speed of neutral helium are shown. From the left to the right, we show the results for the total, pristine, and secondary helium. The orientation of the LISM velocity and ISMF vectors is shown in panel (a). The adopted definition of positive deflection for a generic particle with speed $\boldsymbol{v}_{\rm He}$ is indicated in panel (d).

The presence of the heliotail modifies the ISMF and affects the anisotropy of multi-TeV GCR flux (Schwadron et al., 2014; Zhang et al. 2014; 2016; 2019, 2020)

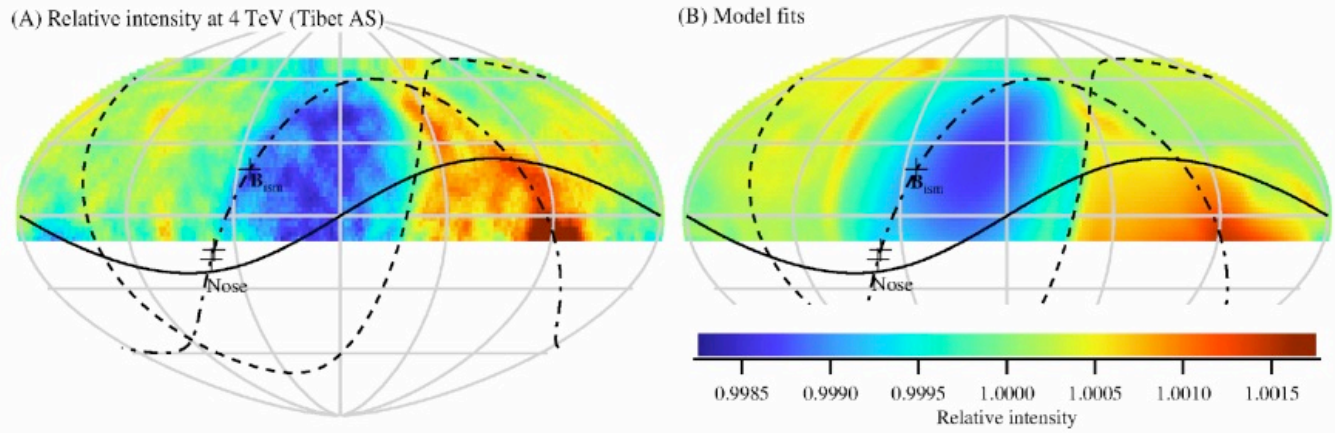

Figure 10: 5°-average anisotropy of 4 TeV CR as measured in the Tibet Air Shower experiment (*left*), the model calculation (*right*). The solid, dashed, and dash-dotted curves show the ecliptic plane, the plane perpendicular to LISM magnetic field and passing through the Sun, and the hydrogen deflection plane, which is also the plane containing the vectors of interstellar flow and magnetic field.

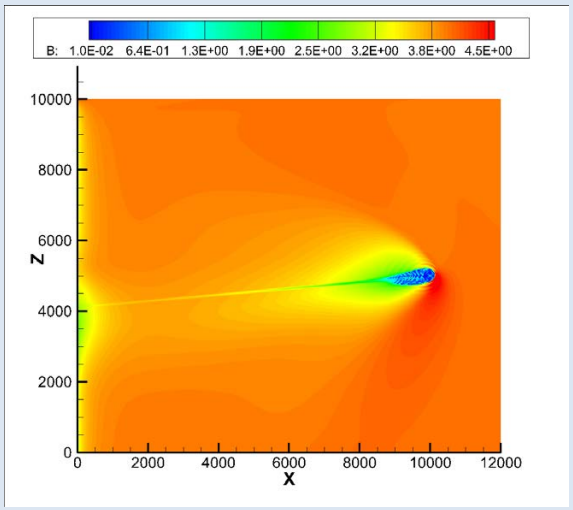

On the left: the distribution of B in the meridional plane

No rotation of the magnetic field vector across the heliopause

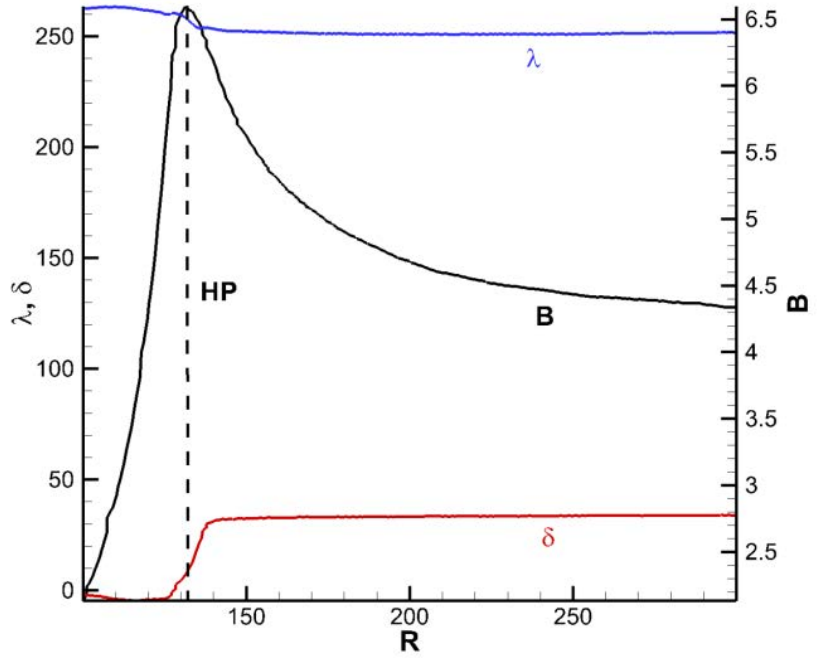

Fig. 1.— Distributions of magnetic field strength, $B = |\mathbf{B}|$, and the elevation and azimuthal angles, δ and λ, along the *V2* trajectory in the SW–LISM interaction assuming unipolar heliospheric magnetic field.

Assumption of the unipolar heliospheric magnetic field (HMF) – obligatory for the "golden croissant" and "curled serpent" solutions - does not reproduce Voyager data even qualitatively. The magnitude of B is highly overestimated. Pogorelov et al. (2017, 2021) agree on that with Izmodenov & Alexashov (2020).

Pogorelov et al. (2015) showed that the heliotail splitting disappears even in the assumption of a flat heliospheric current sheet. Pogorelov et al. (2017) demonstrated that not only the tail splitting, but also the solar wind collimation disappear in the presence of solar cycle, even if in the HMF is unipolar. Korolkov & Izmodenov (2021) showed that there is no heliotail splitting in the assumption of unipolar HMF unless the LISM Mach number is < 0.4.

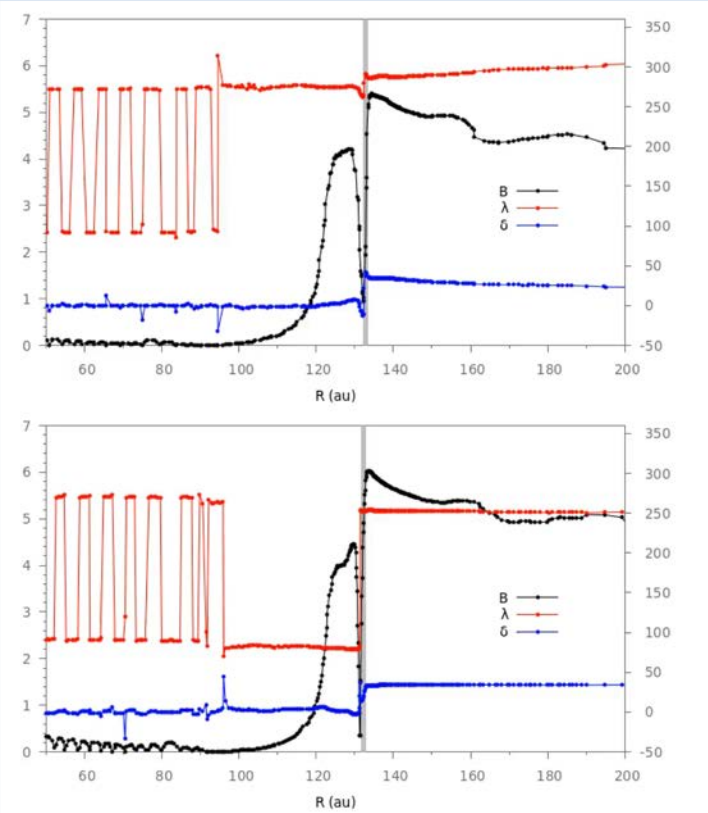

(Left panel) The evolution of B and the azimuthal and elevation angles in the data-driven simulation based on Kim et al. (2017) and extended to 2020. (Right panel) The same in the presence of the HP instabilities (2D figures).
From Pogorelov et al. (2021).

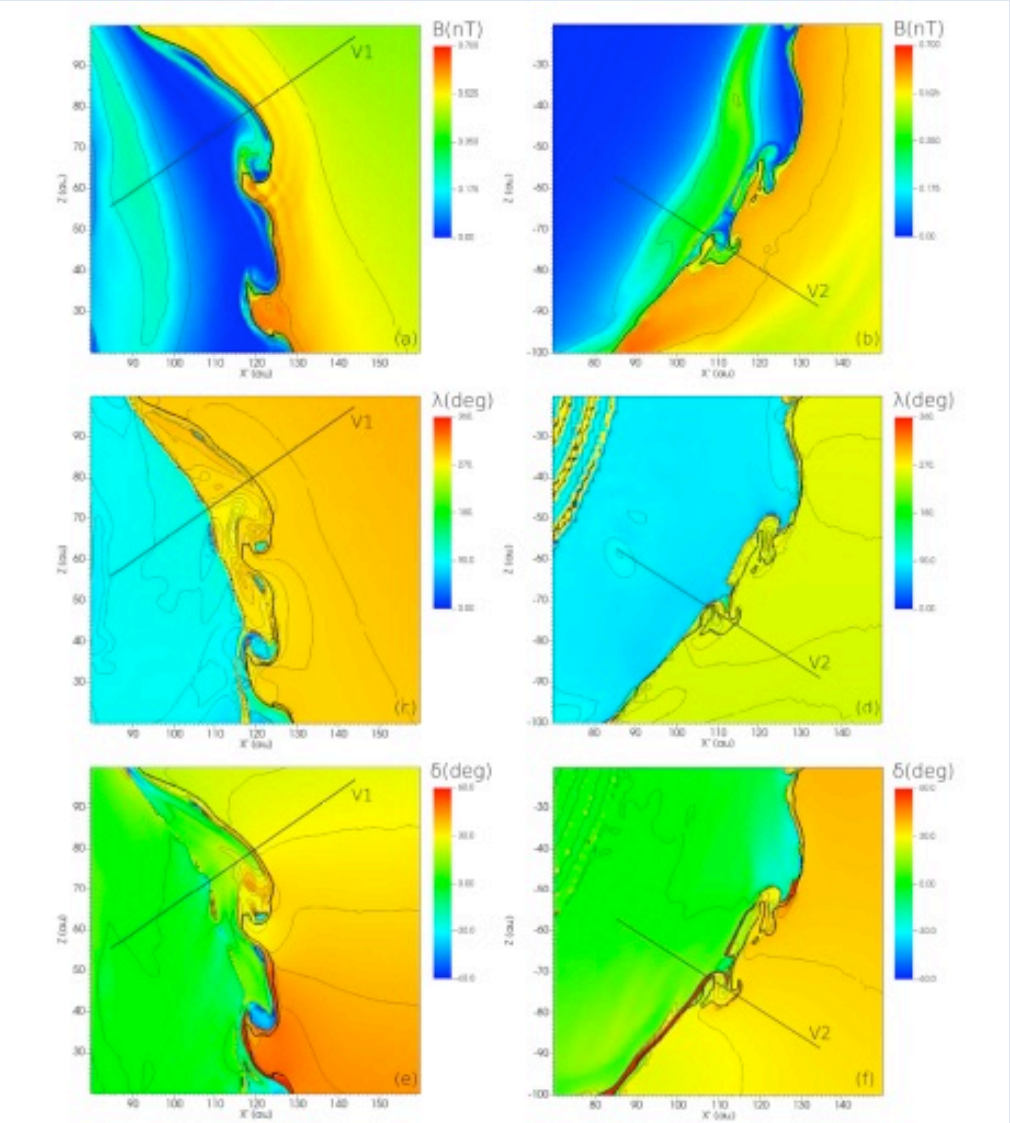

Fig. 2.— Distributions of the magnetic field strength, and the elevation and azimuthal angles (δ and λ) in the planes formed by the z-axis and the $V1$ (left panels) and $V2$ (right panels) trajectories.

No rotation of the magnetic field vector in certain time intervals.

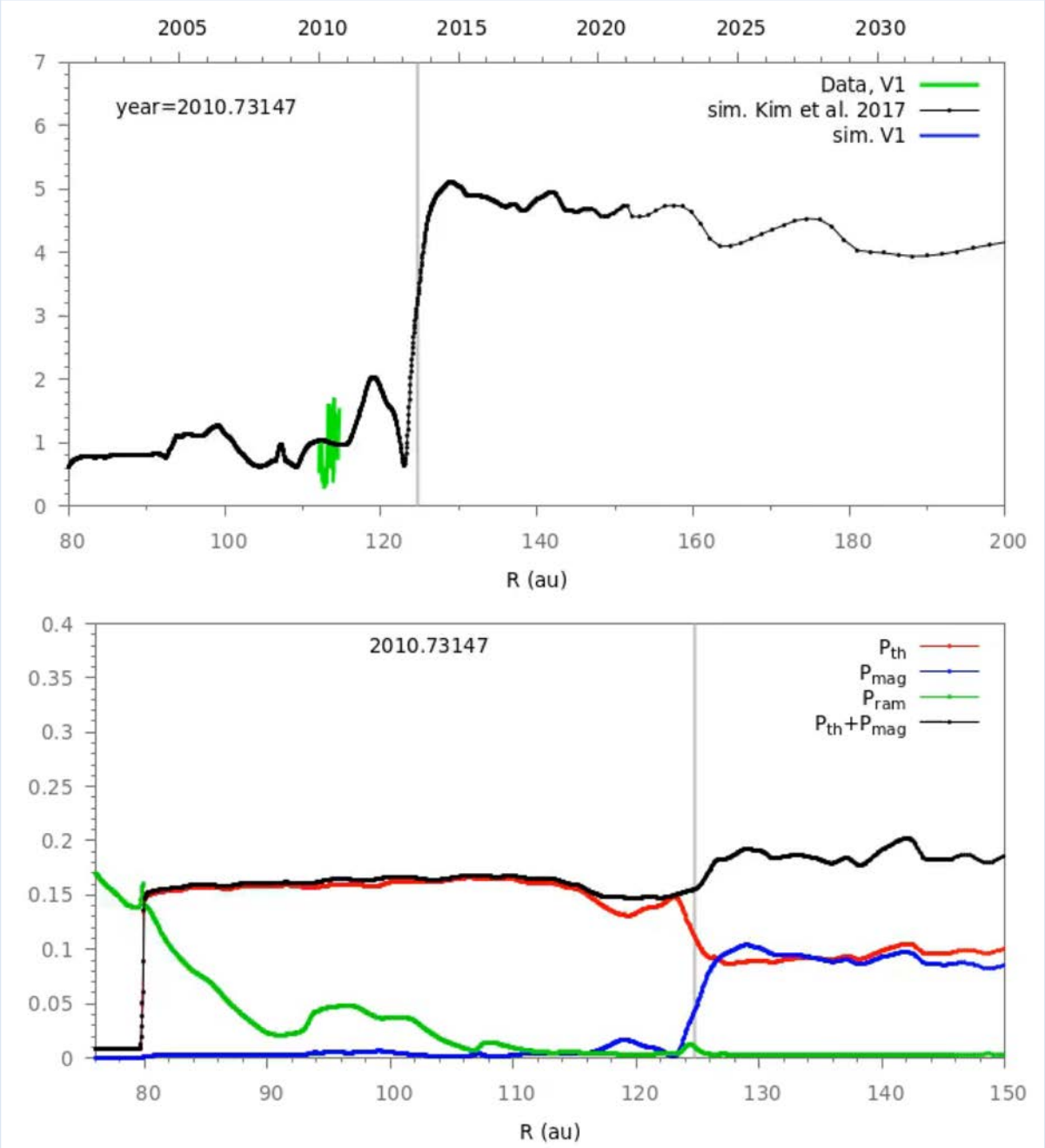

(Top panel) Time evolution of the magnetic field magnitude along the V1 trajectory: data vs 3-D simulations of Kim et al. (2017) extended to 2020.

(Bottom panel) Pressures along the V1 trajectories.

The vertical straight line represents the heliopause.

Notice shock merging. Data-driven simulations show that V1 should start to observe a rather quite flow in the VLISM (see also Burlaga et al., 2020).

Animations from Pogorelov et al. (2021).

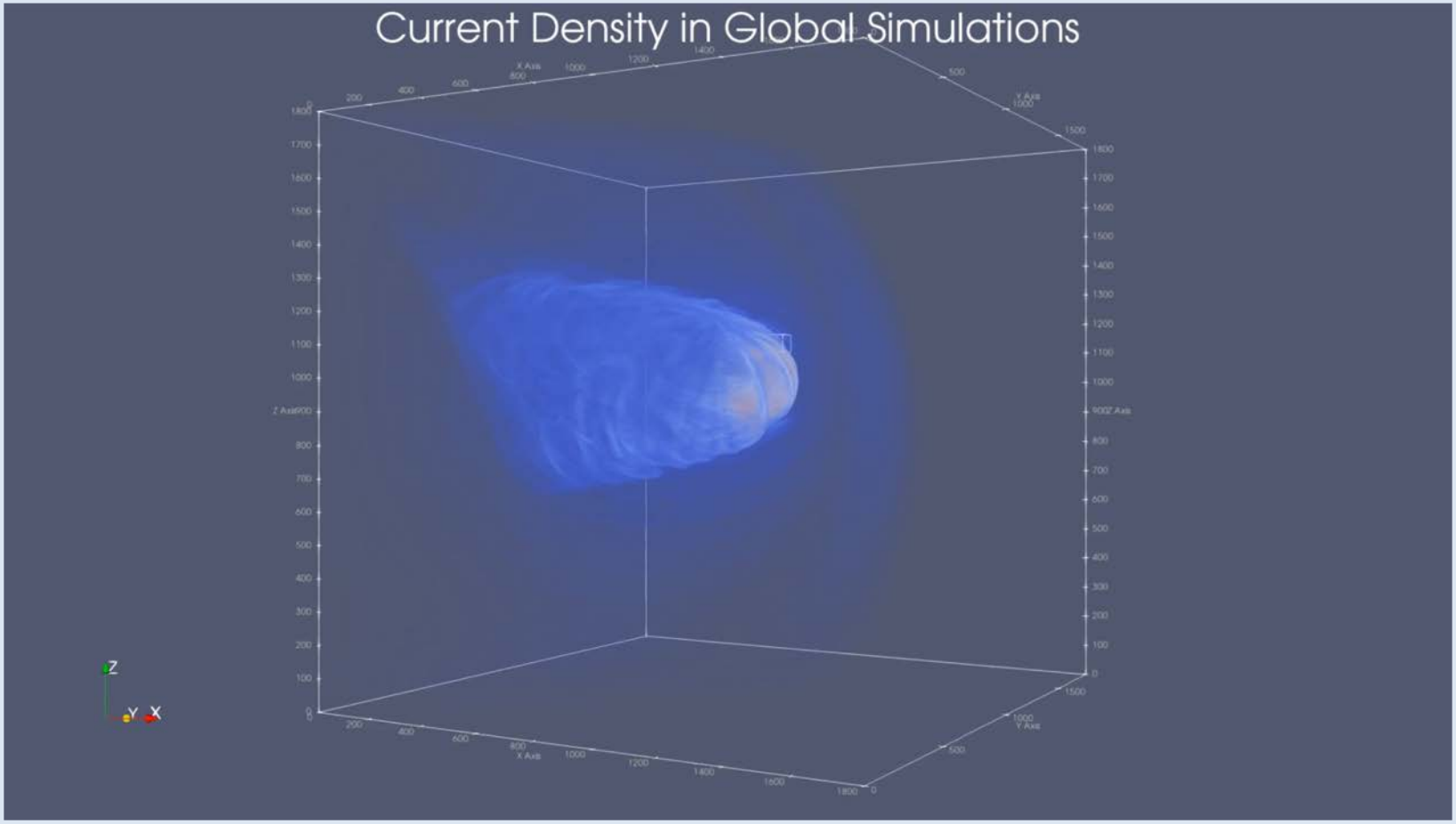

Zoom into the instability/reconnection region on the surface of the heliopause (courtesy of Grzegorz Koval).

More work should be done!